Echolocation signals of free-ranging killer whales (*Orcinus orca*) and modeling of foraging for chinook salmon (*Oncorhynchus tshawytscha*)

Whitlow W. L. Au
Marine Mammal Research Program, Hawaii Institute of Marine Biology, University of Hawaii, Kaneohe, Hawaii 96744

John K. B. Ford
Pacific Biological Station, Fisheries and Oceans Canada, Nanaimo, British Columbia, V9T 6N7 Canada

John K. Horne
School of Aquatic and Fisheries Science, University of Washington, Seattle, Washington

Kelly A. Newman Allman
The Marine Mammal Center, Sausalito, California 94965

(Received 3 April 2003; revised 7 November 2003; accepted 24 November 2003)

Fish-eating "resident"-type killer whales (*Orcinus orca*) that frequent the coastal waters off northeastern Vancouver Island, Canada have a strong preference for chinook salmon (*Oncorhynchus tshawytscha*). The whales in this region often forage along steep cliffs that extend into the water, echolocating their prey. Echolocation signals of resident killer whales were measured with a four-hydrophone symmetrical star array and the signals were simultaneously digitized at a sample rate of 500 kHz using a lunch-box PC. A portable VCR recorded the images from an underwater camera located adjacent to the array center. Only signals emanating from close to the beam axis (1185 total) were chosen for a detailed analysis. Killer whales project very broadband echolocation signals (Q equal 0.9 to 1.4) that tend to have bimodal frequency structure. Ninety-seven percent of the signals had center frequencies between 45 and 80 kHz with bandwidths between 35 and 50 kHz. The peak-to-peak source level of the echolocation signals decreased as a function of the one-way transmission loss to the array. Source levels varied between 195 and 224 dB re:1 μPa. Using a model of target strength for chinook salmon, the echo levels from the echolocation signals are estimated for different horizontal ranges between a whale and a salmon. At a horizontal range of 100 m, the echo level should exceed an *Orcinus* hearing threshold at 50 kHz by over 29 dB and should be greater than sea state 4 noise by at least 9 dB. In moderately heavy rain conditions, the detection range will be reduced substantially and the echo level at a horizontal range of 40 m would be close to the level of the rain noise. © *2004 Acoustical Society of America.* [DOI: 10.1121/1.1642628]

PACS numbers: 43.80.Ev, 43.80.Ka, 43.80.Jz [FD] Pages: 901–909

I. INTRODUCTION

Echolocation experiments with captive dolphins have been conducted since the early 1950's (Schevill and Lawrence, 1953a,b), and yet very little is known about how dolphins utilize their unique echolocation capability in the wild. A variety of detection and discrimination experiments has been conducted (Au, 1993) using a wide assortment of targets including dead fish (Kellogg, 1958), metallic, foam, or plastic spheres, cylinders, and plates. (Au, 1993; Nachtigall and Moore, 1988). For example, an Atlantic bottlenose dolphin (*Tursiops truncates*) can detect a 7.62-cm diameter sphere out to 113 m, in a noisy bay dominated by snapping shrimp (Au and Snyder, 1980). In a quiet environment the detection range for the 7.62-cm sphere would be about 178 m (Au *et al.*, 2002). The echolocation capabilities of dolphins on these "unnatural" objects have provided a wealth of information. Yet we are left with the nagging issue of relevancy of these experiments in understanding how dolphins use echolocation to forage for prey.

One problem with studying echolocation in the wild is the difficulty of obtaining accurate measurements of echolocation signal by free-ranging dolphins. The echolocation beam pattern is relatively narrow and if signals are not measured close to the axis of the animal's beam, the signals will be distorted (Au, 1993). It is also extremely difficult to determine the range between a moving animal and the recording hydrophone. A range determination is essential in order to calculate the source level (sound-pressure level 1 m from the dolphin) of the signals.

These two problems have been successfully overcome by using a short-baseline array of four hydrophones arranged as a symmetrical star (Au and Herzing, 2003; Rasmussen *et al.*, 2002). Such an array geometry has been used successfully by Aubauer (1995) to track flying bats. With this array, a researcher can determine whether a received signal was measured along the major axis of a dolphin's transmission beam as well as estimate the range of the animal from the array.

Killer whales (*Orcinus orca*), found in the coastal waters of British Columbia, Washington State and southeastern

Alaska, are ideal candidates to investigate the details of echolocation signal production in a free-ranging odontocete. This region is inhabited by two distinct ecotypes of the species, each with a different dietary specialization (Ford *et al.*, 2000). The ''transient'' ecotype selectively hunts marine mammal prey, while the ''resident'' ecotype feeds on fishes, particularly salmon. Of the six species of salmon observed to be taken, chinook (*Oncorhynchus tshawytscha*) was the most common, presumably because of their large size and rich lipid content (Ford *et al.*, 1998). Acoustic studies by Barrett-Lennard (1996) have shown that transient killer whales seldom use echolocation signals, likely as a hunting strategy, but resident killer whales frequently emit echolocation clicks while foraging for salmon. In this study, results from echolocation signal measurements of free-ranging resident-type killer whales are presented and these results are incorporated into a model involving *Orcinus* foraging on chinook salmon. This study may be the first to model foraging by echolocating odontocetes.

II. PROCEDURE

A. Acoustic measurement system

A four-hydrophone array with the hydrophones arranged as a symmetrical star was used to measure echolocation signals by killer whales. The array structure resembled the letter ''Y,'' with each arm being 45.7 cm in length and separated by an angle of 120°. The arms of the array are constructed out of 1.27-cm-o.d. polyvinyl chloride (PVC) pipe with a spherical hydrophone connected to the end of each pipe and the cable running through the center of the pipe. Another hydrophone is connected at the geometric center of the ''Y.'' An underwater housing attached to the back of the hydrophone mounting plate contained an amplifier and line driver for each of the hydrophones. A multiconductor cable consisting of five coaxial and two dc power lines connected the array electronics to an adjustable battery operated amplifier-filter box that was housed on a boat. The echolocation signals were acquired using a four-channel analog-to-digital converter controlled by a transportable ''lunch-box'' PC housed on the boat. A CCD video camera in another underwater housing was mounted next to the center hydrophone. Additional details of the measurement system can be found in Au and Herzing (2003).

Data acquisition was achieved using two Gage-1210, 12-bit dual simultaneous sampling data acquisition boards housed in the lunch-box PC via two EISA slots. The data acquisition system sampled at 500 kHz with a pretrigger capability. When the computer signaled the Gage-1210 to collect data, four channels of acoustic signals were simultaneously and continuously digitized. Data channels were logged into separate circular memories on each Gage-1210 board. When an echolocation signal was detected by the center hydrophone, it triggered the data acquisition board. Two hundred pretriggered points and 200 post-trigger points were collected for each channel and downloaded to the computer. A total of 80 clicks could be downloaded for each episode before the data had to be stored in a file on the hard drive. A specially constructed ISA board was also used to measure the time interval between clicks being acquired and to trigger a light-emitting diode to indicate that clicks were being captured and recorded. The interclick interval data were also downloaded and stored on the hard drive. The time of capture (to the closest 18-ms interval of the computer timing system) of each click was also saved and stored on the hard drive. The clock on a portable VCR was synchronized to the computer's clock so that the video images were synchronized with the acoustic data.

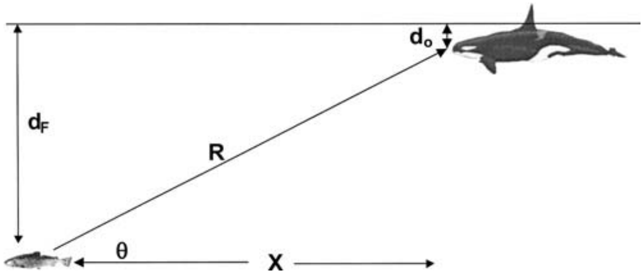

FIG. 1. Foraging geometry showing a killer whale at depth d_o in pursuit of a chinook salmon at range R and a depth d_F.

B. Acoustic measurements

Killer whale echolocation signals were measured on 4 consecutive days in Johnstone Strait, off northeastern Vancouver Island, Canada (50°32′N, 126°42′W) during August, 2000. The four-hydrophone array was deployed from a small boat while small groups of two to three killer whales foraged along the shoreline where rocky cliffs intersect the water at a relatively steep angle. When a group of whales was spotted, the boat would be positioned 150–200 m ahead of and in the path of the animals. The hydrophone array was lowered into the water with the center hydrophone at a depth between 1.2 and 1.5 m. At the same time, an operator controlled the data acquisition sequence by arming the computer to start data acquisition and also started the video tape recorder. As the whales approached the boat, they rarely deviated from their path except to veer to one side if the array was in their path so as to not strike the array.

C. Foraging geometry

In order to examine the use of echolocation by *Orcinus* while foraging on chinook salmon, the geometry in Fig. 1 will be used. In this geometry, the whale is in a pursuit mode directly behind the salmon. The following notations are used in Fig. 1: $\mathbf{d_F}$ and $\mathbf{d_o}$ are the depth of the salmon and the killer whale's sonar, respectively. **R** is the slant range between the fish and the *orca*, **X** is the horizontal range, and θ is the angle between the slant and horizontal range. The angle θ can be determined by the equation

$$\theta=\sin^{-1}\left(\frac{d_F-d_O}{R}\right)=\tan^{-1}\left(\frac{d_F-d_O}{x}\right). \tag{1}$$

The target strength of the salmon is a function of the angle θ, the frequency of the acoustic signal, and the length of the fish (Clay and Horne, 1994). Chinook salmon in Johnstone Strait typically swim at a mean depth of approximately 25 to 64 m during the day (Candy and Quinn, 1999). In this study

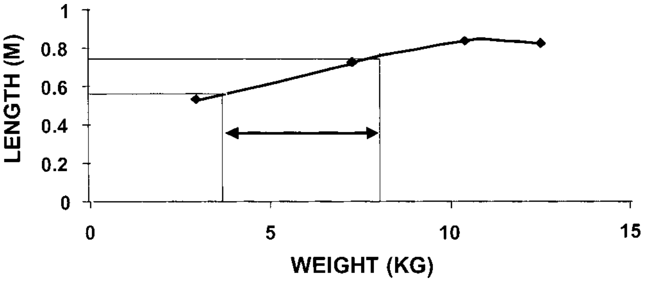

FIG. 2. Comparison of weight versus length for chinook salmon from data provided by Dr. Donald Rogers of the University of Washington.

we assume that the whale is close to the surface during its sonar search, so that a value of 1 m will be used for d_o in Eq. (1).

D. Calculation of salmon target strength

Data collected over a 20-year period in the nearshore waters between Vancouver Island and the mainland British Columbia, and around Queen Charlotte Islands, indicate that chinook salmon are the preferred prey of resident killer whales, during summer (Ford *et al.*, 1998). They also estimated that the preferred weight of the chinook salmon prey was between 3.7 and 8.1 kg. Using length and weight data (unpublished data courtesy of Donald Rogers, U.W., 2002) shown in Fig. 2, the corresponding length of a 3.7-kg chinook salmon is approximately 0.6 m, and 0.8 m for 8.1 kg. A length of 0.78 m will be used in this study.

In order to calculate the strength of an echo returning to an echolocating killer whale, the target strength of chinook salmon must be determined. Clay and Horne (1994) developed a Kirchhoff-ray mode (KRM) backscatter model in which the body of a fish is modeled as a series of short-length fluid-filled cylinders surrounding a set of gas-filled cylinders representing the swimbladder. Backscatter from each cylinder in the body and the swimbladder is estimated and then added coherently to estimate total backscatter as a function of fish length, orientation (i.e., tilt, roll), and acoustic carrier frequency. Model predictions have been shown to match backscatter measurements (Horne and Jech, 1999; Jech and Horne, 2002; Jech *et al.*, 1995). Target strengths of a chinook salmon at 50 kHz were calculated using digitized dorsal and lateral radiographs (Fig. 3) as input to a KRM model parametrized for a 0.78-m caudal length chinook salmon.

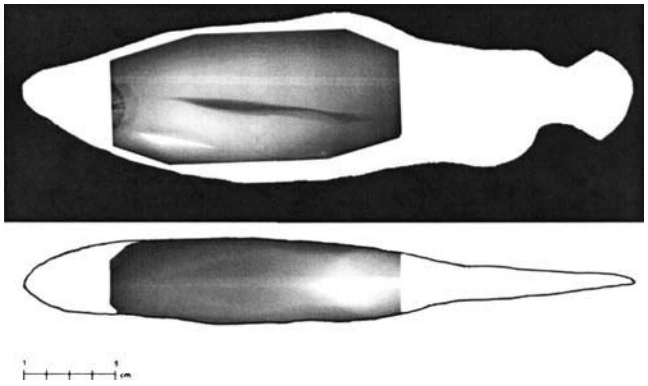

FIG. 3. Radiograph (x-ray images) of a chinook salmon. Top panel is the lateral view and the bottom panel is the dorsal view.

III. RESULTS

A. Echolocation signals

Forty-three files of echolocation clicks were collected during 4 days of measurements. Only echolocation events in which the amplitude of the signals received by the center hydrophone was within 3 dB of the highest were accepted for analysis. These criteria were used to ensure that a killer whale echolocation beam was directed at the array. The beam pattern measured for three different odontocete species (Au, 1993; Au *et al.*, 1995) indicate that when the major axis of the beam is directed to within ±5° of the center hydrophone, the signal received by the center hydrophone will be within 3 dB of the highest amplitude. This 3-dB criterion is valid for ranges of approximately 5 to about 15-m range if a whale's head orientation was along the perpendicular bisect of the array. However, as the whales approached within about 5 to 10 m of the boat, they would totally submerge and swim to the side or below the array to avoid hitting it but still direct their signals towards the array. The whales almost always pointed their head towards the array as they approach the boat so that most of the echolocation clicks collected at short ranges were directed towards the center of the array.

Four spectra of echolocation click trains are shown in Fig. 4 presented in a waterfall format. The spectra suggest that portions of the signals in a click train can be relatively stable in shape, but also include portions that are highly variable and complex. Most of the energy in the spectra is between 20 and 60 kHz, much lower than for spectra of echolocation signals measured for smaller odontocetes in the field (Au and Herzing, 2003; Rasmussen *et al.*, 2002). Most of the clicks had bimodal frequency spectra with both primary and secondary peaks separated by as little as 10–15 kHz. The secondary peaks vary in shape from a slight "bump" in spectra to a clearly defined peak. The frequency of the bumps and distinct peaks were usually at similar frequencies.

Three representative types of clicks are shown in Fig. 5 with the signal waveforms on the right and the frequency spectra on the left. These clicks are very brief, generally between 80 and 120 μs in duration, with broad frequency spectra. The presence of clicks with bimodal spectra is obvious in the spectra plots. The majority (~89%) of the clicks examined had bimodal spectra. The killer whale click waveforms resemble those of other odontocetes such as *Tursiops truncatus, Delphinapterus leucas* (Au, 1993), *Pseudorca crassidens* (Au *et al.*, 1995), *Lagenorhynchus albirostris* (Rasmussen *et al.*, 2002), and *Grampus griseus* (Phillips *et al.*, 2003), but had almost twice as long duration and were almost an octave lower in frequency. Signals with a single high-frequency peak usually associated with higher amplitude signals (Au *et al.*, 1995) were rarely observed.

Orcinus projects relatively high amplitude signals with the maximum peak-to-peak source level measured at about $224\,\mathrm{dB}\,re\!:\!1\,\mu\mathrm{Pa}$. Most of the signals (75%) had source levels between 195 and $210\,\mathrm{dB}\,re\!:\!1\,\mu\mathrm{Pa}$. The peak-to-peak source level as a function of range between an echolocating

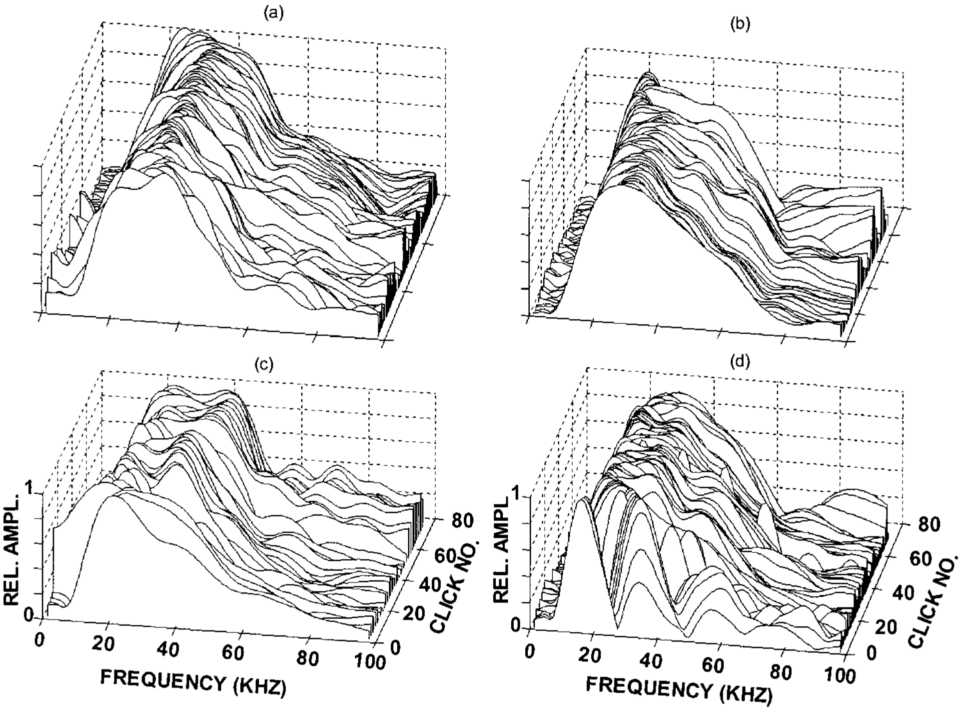

FIG. 4. Examples of the frequency spectra of four *Orcinus orca* echolocation click trains in a waterfall format.

killer whale and the array is shown in Fig. 6. As the whale's range to the array decreased, the source level also decreased. The solid curve in Fig. 6 is a regression curve represented by the equation

$$\mathrm{SL(dB)} = 181.4 + 20\log(R), \tag{2}$$

and has an r^2 value of 0.56, where R is the range in meters. The decrease in source level corresponded to the decrease in the one-way spherical spreading loss. Therefore, the amplitude of the echoes returning to the whales increased in magnitude as the range decreased, suggesting that killer whales prefer to receive echoes that have increasing signal to noise. Figure 6 also suggests that the whales were echolocating on the hydrophone array and not on some other objects, since the source level decreased as the range to the array decreased.

The histogram of center frequency is shown in Fig. 7. Center frequency is defined as that frequency which divides the energy in a frequency spectrum into two equal parts. The peak in the distribution of center frequency shown in the histogram occurred at 50 kHz, with 76% of the signals having center frequencies greater than 50 kHz. For bimodal spectra, center frequency is a better description of the fre-

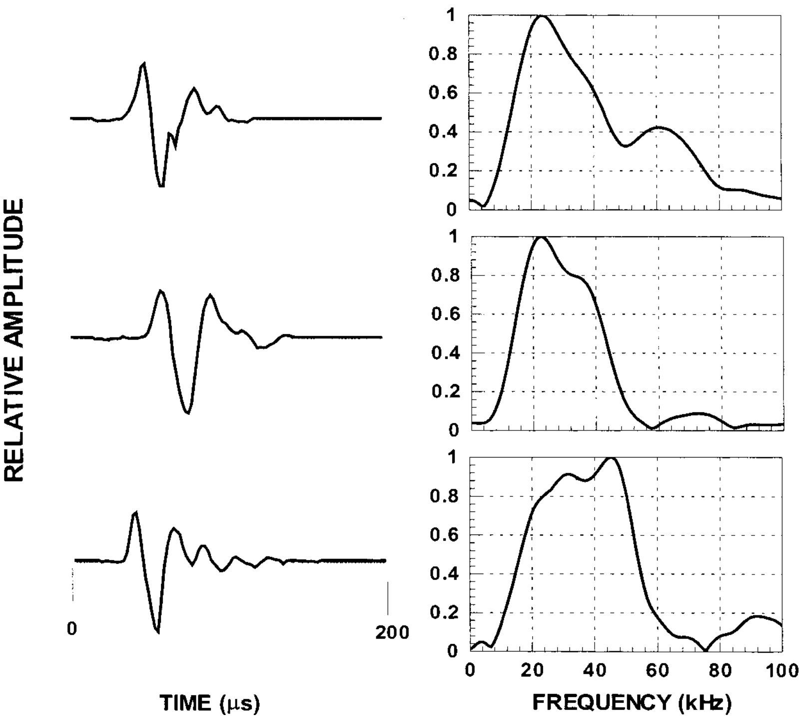

FIG. 5. Examples of the some representative waveforms and frequency spectra emitted by *Orcinus orca* in Johnstone Strait, Canada.

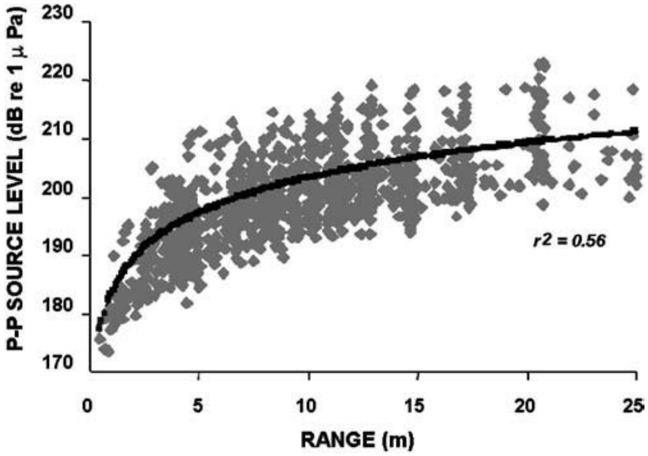

FIG. 6. Peak-to-peak source level as a function of range. The source levels are depicted by the gray diamond symbols. The solid line is the best-fit regression curve represented by the equation $A+20\log R$, where A is a constant and R is the range between a killer whale and the symmetrical star array.

quency spectra than peak frequency (Au *et al.*, 1995). Eighty-nine percent of the echolocation clicks had bimodal spectra in which the amplitude of the secondary peaks were within 50% of the amplitude of the primary peak.

The histogram of rms bandwidth is shown in Fig. 8. The rms bandwidth is a measure of the frequency width of a spectrum about the center frequency. The 3-dB bandwidth for bimodal spectra can often provide a misrepresentation of the width of the signal since the bandwidth might cover only the frequency range about the peak frequency. The rms bandwidth is probably a better measure of the width of signals with bimodal spectra. Most of the signals (83%) had an rms bandwidth between 35 and 50 kHz, with the peak in the histogram at 40 kHz. The Q of a signal is defined as the ratio of the center frequency over the rms bandwidth, and is equal to 0.9 to 1.4 for our data. These Q values indicate that *Orcinus* projects broadband echolocation signals.

B. Salmon target strength

The salmon was modeled using 775 fluid- and 290 gas-filled cylinders representing the body and swimbladder, respectively. Predicted target strength values plotted in three dimensions as a function of the tilt angle θ and the roll angle φ are shown in Fig. 9. KRM-predicted backscatter intensities in the killer whale "attack quadrant" (90° tilt, 180° roll) depend on the orientation of the fish relative to the incident echolocation acoustic wave. Target strengths vary by approximately 40 dB within the attack quadrant, increasing from low values at tail-on incidence to peak values at dorsal incidence. In the roll plane, maximum backscatter occurs at lateral incidence. The ridges and folds are due to constructive and destructive interference between the body and swimbladder at 50 kHz.

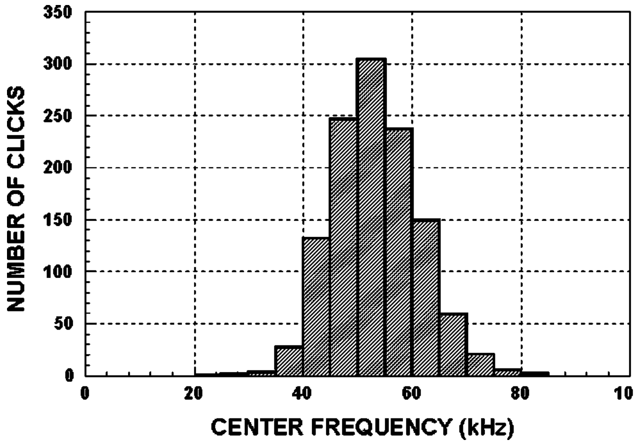

FIG. 7. Histogram of center frequency of echolocation signals.

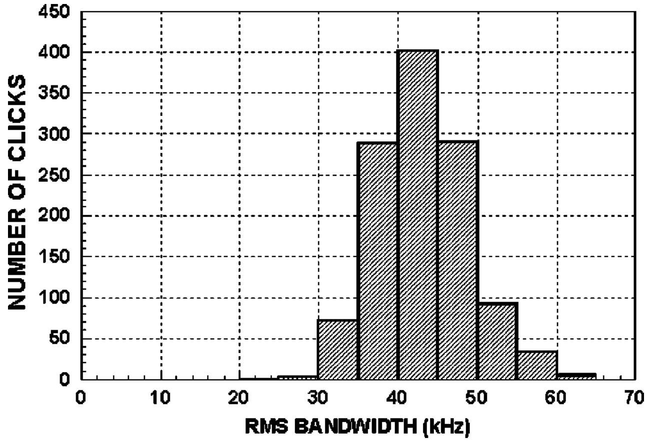

FIG. 8. Histogram of rms bandwidth of echolocation signals.

The target strength along the plane that is passed through the 0° roll of Fig. 9 is shown in Fig. 10. The degree values in Fig. 10 refer to the incident angle θ in the tilt plane, which matches the angle shown in Fig. 1. Also shown in the figure is the five-point moving average of target strength at 50 kHz over a range of 30° to 85°. The five-point moving average process effectively smoothened the target strength

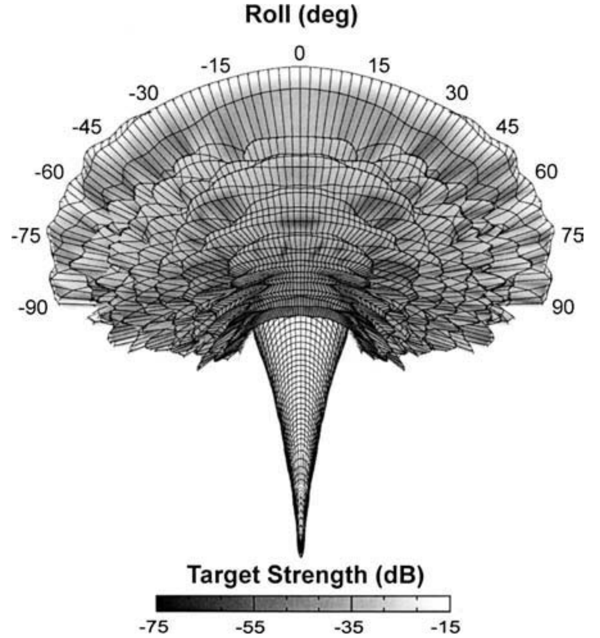

FIG. 9. Predicted Chinook salmon (*Oncorhynchus tshawytscha*) target strength (dB) at 50 kHz viewed at a 45° angle looking toward the head of the fish. KRM backscatter predictions are resolved at 2° in the tilt plane and 2° in the roll plane. Backscatter amplitude is depicted as distance from the center of the fish and using a gray scale where dark is low and white is high.

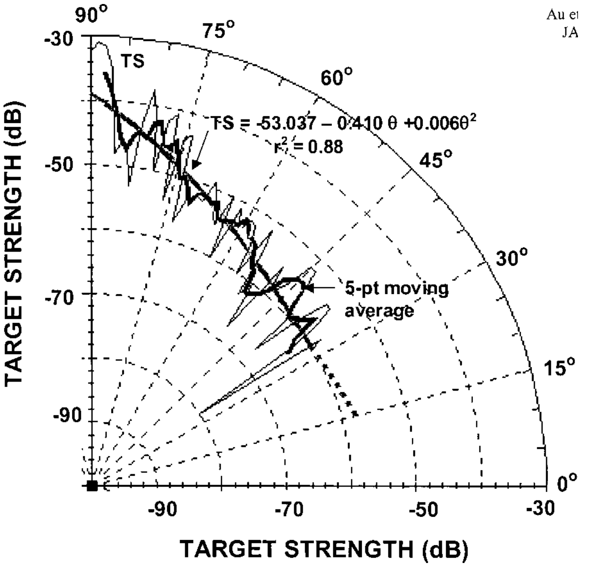

FIG. 10. Polar plot of chinnook salmon (*Oncorhynchus tshawytscha*) predicted target strength in the tilt plane along its spine at a 0° roll angle. The thin, black line is the KRM predicted backscatter at 50 kHz. The thick, black line is a five-point moving average of the target strength, starting at 30°. The gray solid curve is a second-order polynomial curve fit to the moving average.

results and removed the deep nulls. Target strength measurements using broadband, click signals indicate that deep nulls such as those observed in Fig. 10 do not exist (Benoit-Bird *et al.*, 2003). As a killer whale pursues and closes in on a prey, the attack angle between the predator and a prey will continuously change along with the target strength of the prey. A second-order polynomial was fitted to the 5-point moving average target strength curve ($r^2 = 0.88$). The equation for the fitted curve is

$$\mathrm{TS}(\theta) = -53.037 - 0.410 + 0.006\,\theta^2, \tag{3}$$

where θ is the attack angle in degrees and is defined by Eq. (1) depicted in Fig. 1.

C. Calculation of echo level

The level of the echoes (EL) in dB reflecting off a salmon and arriving back to the killer whale can be calculated with the equation

$$\mathrm{EL} = \mathrm{SL} - \mathrm{TL} + \mathrm{TS}, \tag{4}$$

where SL is the peak-to-peak source level, TL is the two-way transmission loss, and TS is the target strength. Substituting Eq. (2) for the SL and Eq. (3) for TS, and assuming spherical spreading loss, the peak-to-peak echo level can be expressed as

$$\mathrm{EL} = 128.633 - 20 \log R - 2\alpha R - 0.410\,\theta + 0.006\,\theta^2, \tag{5}$$

where α is the absorption loss at 50 kHz and is approximately 0.016 dB/m (Urick, 1983). The echo level as a function of horizontal range between the salmon and the killer whale is plotted in Fig. 11 for a salmon depth of 25, 45, and 65 m. The echo levels for different salmon depths are not very different; at 100 m there is only a 4-dB difference between the salmon depth of 25 and 65 m. The differences become smaller for shorter horizontal ranges.

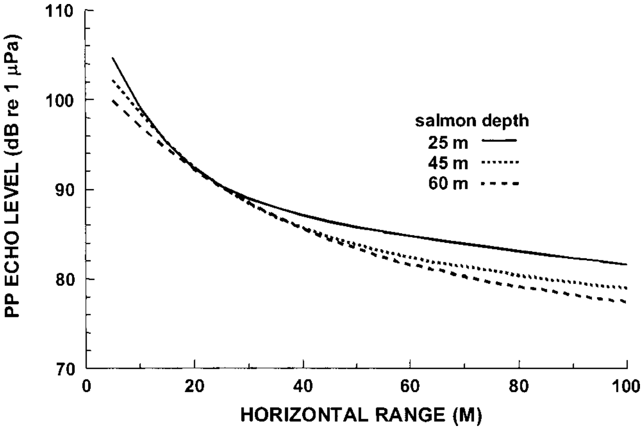

FIG. 11. Estimated peak-to-peak echo level of backscatter from a 0.7-m chinook salmon swiming at a depth of 30–50 m as a function of the horizontal range between the salmon and a foraging killer whale.

D. Detectability in quiet and noisy conditions

The echo levels shown on Fig. 11 can be compared with hearing threshold data for *Orcinus* obtained with a relatively broadband acoustic stimuli. This is important because hearing threshold obtained with narrow-band tonal signals may be different than thresholds obtained with broader band signals (Au *et al.*, 2002). Szymanski (1999) determined the hearing threshold of a killer whale by measuring the auditory brainstem response (ABR) using short tone bursts having durations of 0.5 ms as the acoustic stimuli. Such a short tone burst will have a broadband characteristic. ABR thresholds of 48 dB *re* 1 μPa peak-to-peak, for a 45-kHz tone burst and 52 dB for a 60-kHz tone burst were measured. Using a linear interpolation, the ABR threshold at 50 kHz should be approximately 49 dB. At a horizontal range of 100 m between a killer whale and a chinook salmon prey, the echo levels should vary between 82 and 78 dB for a salmon depth of 25 and 65 m, respectively. Therefore, in a quiet environment an echolocating killer whale would receive echoes that are between 29 and 33 dB above the ABR threshold at a horizontal range of 100 m. The echo levels shown in Fig. 11 taper off slowly, with range beyond 100 m suggesting the detection range probably extends considerably beyond 100 m. At the present time it is uncertain what would be considered the maximum range at which a killer whale would attack a prey, so we hesitate to extrapolate to longer ranges.

Under conditions in which an *Orcinus*' hearing is masked by ambient noise, the received echo level will be the same as in Fig. 11, but the received noise must also be considered in order to estimate detection ranges. The amount of noise (NL) that an animal will receive into its auditory system can be expressed as

$$\mathrm{NL} = N_0 + \mathrm{BW} - \mathrm{DI}, \tag{6}$$

where N_0 is the noise spectral density of the ambient noise, BW is the received bandwidth, and DI is the directivity index of the animal's auditory system. The receive bandwidth is a difficult parameter to deal with since the transmitted signal is broadband, so that echoes produced by the signal will also be broadband and probably cover several critical bands of the animal's auditory system. One way of overcoming this difficulty is to use the rms bandwidth of the transmitter signal. From the histogram of Fig. 8, most of the signals had an rms bandwidth between 35 and 50 kHz. If we choose a 40-kHz bandwidth, then the bandwidth in dB will be

$$\mathrm{BW}=10\log(40\ \ \mathrm{kHz})=46\ \ \mathrm{dB}. \tag{7}$$

The only odontocete in which the receiving beam pattern has been measured and the receiving directivity index estimated is *Tursiops* (Au and Moore, 1984). At 50 kHz, DI is approximately equal to 11 dB. The receiving directivity index for a killer whale can be estimated by modeling the sound-receiving system of both species using a circular disk transducer. The receiving directivity index for a circular transducer at a specific frequency is proportional to the radius, i.e., the larger the radius the larger the directivity index. Using the same line of reasoning with the killer whale, its receiving directivity index will be larger than that of the bottlenose dolphin (Au *et al.*, 1999). Therefore, the directivity index for a killer whale can be estimated by using the equation

$$\mathrm{DI}_{\mathrm{OO}}=\mathrm{DI}_{\mathrm{TT}}+20\log\left(\frac{a_{\mathrm{OO}}}{a_{\mathrm{TT}}}\right), \tag{8}$$

where $\mathrm{DI}_{\mathrm{OO}}$ is the directivity index for *Orcinus*, $\mathrm{DI}_{\mathrm{TT}}$ is the directivity index for *Tursiops*, a_{OO} is the radius of an killer whale's head, and a_{TT} is the radius of a *Tursiops* head measured at the blow hole. The ratio of $\mathrm{a}_{\mathrm{OO}}/\mathrm{a}_{\mathrm{TT}}$ varies between 3 and 3.5. If we use a ratio of 3, the directivity index for an *Orcinus* at 50 kHz will be approximately 10 dB larger than that of *Tursiops*, or 21 dB. Let us assume a sea state 4 condition, in which the noise spectral density at 50 kHz is approximately $35\,\mathrm{dB}\,re{:}1\ \mu\mathrm{Pa}^2/\mathrm{Hz}$ (Urick, 1983). Therefore, from Eq. (6) the received noise level centered at 50 kHz will be approximately 60-dB rms. Since the source level in Eq. (4) and the ABR threshold are given in terms of peak-to-peak sound-pressure levels, the received noise should also be expressed in terms of its peak-to-peak value. Using the relationship between the rms and peak-to-peak values of a sine wave, we merely add 9 dB to the rms value and obtain a peak-to-peak noise level in the frequency band centered at 50 kHz of 69 dB. Therefore, even in sea state 4, the echo level from a chinook salmon would be at least 9 dB above the received noise level at a horizontal range of 100 m.

Another source of ambient noise besides wind and wave is falling rain. Rain can increase the ambient noise level considerably, depending on the rate of precipitation and sea state conditions (Scrimger *et al.*, 1989). For rain fall of 3 mm/hr, the rms noise spectral level at 50 kHz is approximately 42 dB, which is only 7 dB above sea state 4 noise level (Urick, 1983). The received echo should be at least 2 dB above the rain noise at a horizontal range of 100 m and increase rapidly for shorter horizontal ranges. However, for moderately heavy rain the rms noise spectral level will increase to approximately $52\,\mathrm{dB}\,re{:}1\ \mu\mathrm{Pa}^2/\mathrm{Hz}$ (Urick, 1983) so that the horizontal range must be shorter than about 40 m before the signal begins to extend above the noise level. The situation will not be as drastic as it seems since rain noise originates at the surface, and if the *Orcinus*' beam is pointed below the horizon the received noise will be less than predicted by Eq. (6). The use of the directivity index in Eq. (6) assumes that the noise is isotropic (Urick, 1983) and can only be used to obtain a rough estimate of the received anisotropic rain noise. Nevertheless, under moderately heavy rain conditions, the detection range of *Orcinus* may be reduced significantly but probably not enough to prevent it from foraging by echolocation. Furthermore, the whale might change hunting tactics and swim some depth below the surface in order to avoid the rain noise at the surface.

IV. DISCUSSION AND CONCLUSIONS

Orcinus projects broadband, short-duration echolocation signals similar to those of other odontocetes. The signals are brief, with only three to seven oscillations, and broadband with a Q between 0.9 and 1.4. The signals have a duration that is approximately twice as long as those used by *Tursiops* and other small odontocetes (Au, 1993), with a center frequency lower by close to one octave. Most of the signals have a bimodal frequency distribution which contributes to the broadband nature of the signals. The bimodal distribution has a low-frequency peak between 20 and 30 kHz and a high-frequency peak between 40 and 60 kHz, with the peak in the center frequency histogram at 50 kHz. The broad bandwidth of the echolocation signal provides a good range resolution capability (Au, 1993) that should enable *Orcinus* to perform fine target discrimination, especially close to where the rocky cliff protrudes steeply into the water in Johnstone Strait. Salmon have been known to seek refuge along the cliffs in this area from foraging killer whales (Ford *et al.*, 1998).

The peak-to-peak source levels measured for *Orcinus* are comparable to those measured for *Tursiops* in open-water captive echolocation experiments (Au, 1993; Au and Snyder, 1980) for comparable target ranges. For target ranges between 6 and 20 m, *Tursiops* source levels varied from about 204 to $216\,\mathrm{dB}\,re{:}1\ \mu\mathrm{Pa}$, which is similar to that of *Orcinus*. However, there is a large difference between the target strength of targets used in the echolocation experiments with *Tursiops* and the target strength of the array assembly used to measure signals in the field. Although the target strength of the array was not measured, the theoretical target strength of an aluminum pipe, connected to a flat Plexiglas container mounted on a flat delrin plate along with a camera holder, should be approximately 15–20 dB greater than the small cylinders and spheres used in the *Tursiops* experiments (Au, 1993; Au and Snyder, 1980). The fact that the amplitude of echolocation signals used by free-ranging dolphins is comparable to those used by captive dolphins suggests the importance of range on the source levels utilized by dolphins. Despite the higher target strength of the array, the killer whale emitted similar source levels as *Tursiops* echolocating on much weaker targets at similar ranges.

The amplitude of the echolocation signals is sufficiently high for the killer whales to detect chinook salmon prey at relatively long ranges (≈100 m) in the presence of relatively high wind and wave conditions. Refined estimates of echo levels and detection ranges can be obtained by further research on the echolocation and auditory capabilities of *Orcinus*, and on broadband backscatter from salmon and other fishes. Some parameters that need to be obtained for *Orcinus* include the echolocation detection threshold in quiet and in noise, receiving directivity index, and receiving bandwidth applicable to echolocation. Models of acoustic backscatter from fishes with a swimbladder for broadband, short-duration signals also need to be developed. The echo levels obtained in this study are based on the estimates of missing or unknown parameters pertaining to both the killer whale and salmon. Despite the presence of certain unknowns, it is doubtful that the results of this study would be significantly altered if all the parameters were known. The echo level at a horizontal range of 100 m is sufficiently high that slight adjustments in the echo level would probably not have any consequence. The pursuit geometry in which a prey is swimming directly away from the predator used in this study resulted in relatively low target strength values for the chinook salmon. Higher target strength can be expected for a geometry in which the longitudinal axis of a salmon is close to being perpendicular to the trajectory of the echolocation signal emitted by a killer whale. Here, we assume that the *Orcinus*' head is oriented so that the acoustic axis of its sonar system is pointed directly at the prey.

An interesting issue that has arisen as the result of this study is associated with the range at which a killer whale predator would consider a chinook salmon as a prey worth pursuing. The amount of energy that a predator must expend in order to close the distance between it and the prey can be assumed to be directly proportional to the distance between it and the prey. Just because an *Orcinus* can detect a chinook salmon at ranges in excess of 100 m does not necessarily mean that it will start pursuing that salmon from that range. There is a good possibility that the predator would continue to hunt for a prey that would be at a closer range. It is also likely that the whale may continue swimming in the direction of a salmon until the separation distance closes to a particular limit before it begins a pursuit of the prey. Unfortunately, little is known on this important and interesting topic.

There is also the issue of the prey possibly hearing the echolocation signals of a predator killer whale. Unfortunately, there is little information on the hearing characteristics of salmon. Hawkins (1978) measured the audiogram of an Atlantic salmon (*Salmo salar*) and found an upper frequency of hearing of approximately 400 Hz. We should not expect much difference in the upper limit of hearing for other salmon species. Therefore, we could surmise that it would be very unlikely for a Chinook salmon to detect the echolocation signals of a foraging killer whale.

The foraging behavior of *Orcinus* in the vicinity of Vancouver Island pursuing individual salmon is in contrast to the foraging behavior of killer whales feeding on herring in Norway (Nottestad *et al.*, 2002). A herring school would present a much larger target strength than an individual salmon. The target strength of a school would probably not depend on the direction from which a sonar signal arrives. Therefore, the detection range should be greater with a school and it would not depend strongly on the orientation of the killer whale with respect to the school.

This is the first study to model prey detection by echolocation for any odontocete. Although certain assumptions associated with the killer whale's echolocation and auditory systems were made, based on studies on the Atlantic bottlenose dolphins, we feel that the results obtained are representative of the *Orcinus orca*. Our results suggest that killer whales foraging on chinook salmon in coastal waters of British Columbia are well equipped to detect their prey at ample ranges to be successful at the task.

ACKNOWLEDGMENTS

We thank James and Mary Borrowman of Stubbs Island Whale Watching, Telegraph Cove, British Columbia, for use of their skiff and for hosting us. We also thank Graeme Ellis for the use of his boat and for his assistance. This study was supported in part by the Office of Naval Research, Grant No. N00014-99-1-0800 to Paul E. Nachtigall and Whitlow Au, from Dr. Robert Gisiner, Program Manager. Support for the fish backscatter research came from ONR's Biological/Chemical Oceanography, Ocean Acoustics Science Divisions. The support of the Vancouver Aquarium Marine Science Centre is also appreciated. This is HIMB contribution No. 1170.

Au, W. W. L. (**1993**). *The Sonar of Dolphins* (Springer, New York).

Au, W. W. L., and Herzing, D. L. (**2003**). "Echolocation signals of wild Atlantic spotted dolphin (*Stenella frontalis*)," J. Acoust. Soc. Am. **113**, 598–604.

Au, W. W. L., Kastelein, R. A., Ripper, T., and Schooneman, N. M. (**1999**). "Transmission beam pattern and echolocation signals of a harbor porpoise (*Phocoena phocoena*)," J. Acoust. Soc. Am. **106**, 3699–3705.

Au, W. W. L., Lemonds, D. W., Vlachos, S., Nachtigall, P. E., and Roitblat, H. L. (**2002**). "Atlantic bottlenose dolphin hearing threshold for brief broadband signals," J. Comp. Psychol. **116**, 151–157.

Au, W. W. L., and Moore, P. W. B. (**1984**). "Receiving beam patterns and directivity indices of the Atlantic bottlenose dolphin, *Tursiops truncatus*," J. Acoust. Soc. Am. **75**, 255–262.

Au, W. W. L., Pawloski, J. L., Nachtigall, P. E., Blonz, M., and Gisner, R. C. (**1995**). "Echolocation signals and transmission beam pattern of a false killer whale (*Pseudorca crassidens*)," J. Acoust. Soc. Am. **98**, 51–59.

Au, W. W. L., and Snyder, K. J. (**1980**). "Long-range target detection in open waters by an echolocating Atlantic bottlenose dolphin," J. Acoust. Soc. Am. **56**, 1280–1290.

Aubauer, R. (**1995**). *Korrelationsverfahren zur Flugbahnverfolgung echoortender Fledemause*, Unpublished Dipl.-Ing, Technishen Hochschule Darmstadt, Darmstadt.

Barret-Lennard, L. G., Ford, J. K. B., and Heise, K. A. (**1996**). "The mixed blessing of echolocation: Differences in sonar use by fish-eating and mammal-eating killer whales," Anim. Behav. **51**, 553–565.

Benoit-Bird, K. J., Au, W. W. L., and Kelley, C. D. (**2003**). "Acoustic backscattering by Hawaiian Lutjanid snappers. I. Target strength and swimbladder characteristics," J. Acoust. Soc. Am. **114**, 2757–2766.

Candy, J. R., and Quinn, T. P. (**1999**). "Behavior of adult chinook salmon (*Oncorhynchus tshawytscha*) in British Columbia coastal waters determined from ultrasonic telemetry," Can. J. Zool. **77**, 1161–1169.

Clay, C. S., and Horne, J. K. (**1994**). "Acoustic models of fish: The Atlantic cod (*Gadus morhua*)," J. Acoust. Soc. Am. **96**, 1661–1668.

Ford, J. K. B., Ellis, G. M., and Balcomb, K. C. (**2000**). *Killer Whales: The Natural History and Genealogy of Orcinus orca in British Columbia and Washington* (UBC Press and U. of Washington Press, Vancouver, B.C., and Seattle, WA).

Ford, J. K. B., Graeme, E. M., Barrett-Lennard, L. G., Morton, A. B., Palm, R. S., and Balcomb III, K. C. (**1998**). "Dietary specialization in two sympatric populations of killer whales (*Orcinus orca*) in coastal British Columbia and adjacent waters," Can. J. Zool. **76**, 1456–1471.

Hawkins, A. D., and Johnstone, A. D. F. (**1978**). ''The hearing of the Atlantic salmon *Salmo salar*,'' J. Fish Biol. **13**, 655–673.

Horne, J. K., and Jech, J. M. (**1999**). ''Multi-frequency estimates of fish abundance: Constraints of rather high frequencies,'' ICES J. Mar. Sci. **56**, 1054–1199.

Jech, J. M., and Horne, J. K. (**2002**). ''Three-dimensional visualization of fish morphometry and acoustic backscatter,'' ARLO **3**, 35–40.

Jech, J. M., Schael, D. M., and Clay, C. S. (**1995**). ''Application of three sound scattering models to threadfin shad (*Dorosoma petenense*),'' J. Acoust. Soc. Am. **98**, 2262–2269.

Kellogg, W. N. (**1958**). ''Echo ranging in the porpoise,'' Science **128**, 982–988.

Nachtigall, P. E., and Moore, P. W. B. (Eds.) (**1988**). *Book Animal Sonar: Processes and Performance* (Plenum, New York).

Nottestad, L., Misund, O. A., Ferno, A., Melle, W., Mackinson, S., Axelsen, B., and Pitcher, T. (**2002**). ''Synoptic field studies of Norwegian spring-spawning herring: Acoustics, Behaviour and Ecology,'' Paper presented at the ICES Symposium of Acoustics in Fisheries and Aquatic Ecology, Montpellier, France, 10–14 June, 2002.

Phillips, J. D., Nachtigall, P. E., Au, W. W. L., Pawloski, J. L., and Roitblat, H. L. (**2003**). ''Echolocation in Risso's dolphin (*Grampius griseus*),'' J. Acoust. Soc. Am. **113**, 605–616.

Rasmussen, M. H., Miller, L. A., and Au, W. W. L. (**2002**). ''Source levels of clicks from free-ranging white beaked dolphins (*Lagenorhynchus albirostris* Gray 1846) recorded in Icelandic waters,'' J. Acoust. Soc. Am. **111**, 1122–1125.

Scheville, WE, and Lawrence, B. (**1953a**). ''Auditory response of a bottlenose porpoise, Tursiops turncatus, to frequencies above 100 Kc.'' J. Exp. Zool. **124**, 147–165.

Scheville, W., and Lawrence, B. (**1953b**). ''High-frequency auditory response of a bottlenosed porpoise, *Tursiops truncatus*, (Montague).'' J. Acoust. Soc. Am. **25**, 1016–1017.

Scrimger, J. A., Evans, D. J., and Yee, W. (**1989**). ''Underwater noise due to rain—open ocean measurements,'' J. Acoust. Soc. Am. **85**, 726–731.

Szymanski, M. D., Bain, D. E., Kiehi, K., Pennington, S., Wong, S., and Henry, K. R. (**1999**). ''Killer whale (*Orcinus orca*) hearing: Auditory brainstem response and behavioral audiograms,'' J. Acoust. Soc. Am. **106**, 1134–1141.

Urick, R. J. (**1983**). *Principles of Underwater Sound* (McGraw-Hill, New York).